

Role of bond-length mismatch in $L_{2-x}\text{Ce}_x\text{CuO}_4$ (L = lanthanide)

Y. T. Zhu and A. Manthiram

Center for Materials Science and Engineering, ETC 9.104, The University of Texas at Austin, Austin, Texas 78712

(Received 19 August 1993; revised manuscript received 15 October 1993)

The electron-doped $L_{2-x}\text{Ce}_x\text{CuO}_4$ (L = lanthanide) superconductors have intergrowth structures in which CuO_2 sheets alternate with $(L,\text{Ce})_2\text{O}_2$ fluorite layers along the c axis. Stabilization of such intergrowth structures requires bond-length matching between Cu-O and (L,Ce) -O bonds. Any bond-length mismatch will result in the buildup of compressive or tensile stresses in the Cu-O and (L,Ce) -O bonds. The consequences of such internal stresses in $L_{2-x}\text{Ce}_x\text{CuO}_4$ are investigated by a systematic variation through L^{3+} size of the lattice parameter a . A decrease in the degree of bond-length mismatch or internal stresses with decreasing L^{3+} size causes a systematic decrease in the Ce solubility limit and in the ease with which oxygen vacancies can be created. The concentration of oxygen vacancies decreases—or the oxygen content increases—with decreasing L^{3+} size for a given N_2 -annealing temperature and Ce content; it also decreases with increasing Ce content for a given L^{3+} ion. The decreasing oxygen-vacancy concentration with decreasing size of L^{3+} causes an apparent increase in the critical Ce concentration x_c required to induce the antiferromagnetic semiconductor to superconductor transition as the size of L^{3+} decreases, although the transition seems to occur at a fixed critical electron concentration $n_c = 0.175 \pm 0.005$ irrespective of the L^{3+} size.

I. INTRODUCTION

Extensive investigation of the copper oxide superconductors during the past few years has led to a recognition of several important crystal-chemical features in these materials. Excepting the infinite-layer compound $\text{Sr}_{1-x}\text{La}_x\text{CuO}_2$ (L = lanthanide),^{1,2} they all have intergrowth structures in which the superconductively active CuO_2 sheets alternate with other, inactive layers along the c axis. For example, a single CuO_2 sheet alternates with double LaO-LaO rocksalt layers along the c axis in the T structure of La_2CuO_4 . The stabilization of such an intergrowth structure requires bond-length matching across the intergrowth interface.^{3,4} The degree of bond-length matching between the intergrowth layers is expressed generally in terms of the Goldschmidt tolerance factor,

$$t = (r_{\text{La}^{3+}} + r_{\text{O}^{2-}}) / \sqrt{2}(r_{\text{Cu}^{2+}} + r_{\text{O}^{2-}}), \quad (1)$$

where $r_{\text{La}^{3+}}$, $r_{\text{Cu}^{2+}}$ and $r_{\text{O}^{2-}}$ refer to room-temperature ionic radii.⁵ A deviation from unity of the value of t produces a bond-length mismatch between the intergrowth layers and results in a buildup of internal stresses in the layers.

A room-temperature tolerance factor $t = 0.87$ in La_2CuO_4 results in a compressive stress in the Cu-O bonds and a tensile stress in the La-O bonds. On the other hand, direct electrostatic repulsion between the negatively charged O^{2-} ions of the fluorite $L\text{-O}_2\text{-L}$ layers in the T' structure of La_2CuO_4 increases the a lattice parameter, which results in a tensile stress in the Cu-O bonds and a compressive stress in the L -O bonds. The presence of compressive vs tensile stresses in the Cu-O bonds of the T and T' structure determines the p - vs n -

type doping.^{3,4}

We had shown^{6,7} by investigating the $\text{La}_{2-x}\text{Nd}_x\text{CuO}_4$ system that the T' structure can be stabilized up to a maximum room-temperature tolerance factor $t \approx 0.858$ ($a \approx 3.97$ Å and Cu-O bond length ≈ 1.985 Å) at $x \approx 1.2$, if the samples are synthesized at 1050°C. Lowering of the synthesis temperature to about 500°C extends the stability of the T' phase to a higher room-temperature tolerance factor $t \approx 0.867$ at $x \approx 0.4$. The shift in the T' phase field to higher x values as the synthesis temperature increases is a consequence of the temperature dependence of the tolerance factor. The tolerance factor t increases as the synthesis temperature increases because of a larger thermal expansion of the (La,Nd) -O bonds compared to that of the Cu-O bonds. An increasing t favors the rock-salt arrangement—i.e., the T structure of La_2CuO_4 —as the synthesis temperature increases. For example, for a given value of $x = 0.5$, the T' structure is found for a lower synthesis temperature $T \leq 600^\circ\text{C}$ while the T structure is encountered for a higher synthesis temperature $T \approx 800^\circ\text{C}$.

Extension of the T' phase field to large $L = \text{Nd}_{1-y}\text{La}_y$ allowed us to synthesize electron-doped $\text{LaNd}_{1-x}\text{Ce}_x\text{CuO}_4$ superconductors.⁸ We found, in agreement with Tao *et al.*,⁹ that the transition from antiferromagnetic semiconductor to superconductor occurs at a smaller $x \approx 0.10$ in the $\text{LaNd}_{1-x}\text{Ce}_x\text{CuO}_4$ system compared to that at $x \approx 0.14$ in $\text{Nd}_{2-x}\text{Ce}_x\text{CuO}_4$ as observed by several groups^{9–11} and by us. We attributed this difference at that time to an increasing Madelung energy caused by a decreasing Cu-O bond length as the L^{3+} size decreases. In order to further identify the origin of such an observed difference, we have now systematically investigated several $\text{La}_{2-x}\text{Ce}_x\text{CuO}_4$ systems with varying Cu-O bond lengths. We find that the variation with L^{3+}

size of internal stresses introduced by bond-length mismatch plays a critical role in determining the Ce solubility, oxygen content, and superconductive properties. We present in this paper the role of bond-length mismatch in the properties of $L_{2-x}Ce_xCuO_4$.

II. EXPERIMENT

The $L_{2-x}Ce_xCuO_4$ samples were prepared by a coprecipitation technique⁶ in order to ensure homogeneity and a uniform distribution of Ce. Required quantities of predried L_2O_3 , ceric ammonium nitrate, and Cu metal were dissolved in dilute nitric acid. A solution of potassium carbonate was then added until the pH was raised to 7 to coprecipitate L^{3+} , Ce^{4+} , and Cu^{2+} as carbonates. The coprecipitate was washed with water, dried at 100°C, and fired in air at 500°C for 6 h. The resulting black powder was ground, pelletized, and fired at 1000°C for 24 h. The pellets were ground, repelletized, and refired at 1000°C for another 24 h. Some $L_{2-x}Ce_xCuO_4$ samples were also synthesized by standard solid-state procedures. Required quantities of L_2O_3 , CeO_2 , and CuO were fired first at 900°C for 20 h and then at 1050°C for 48 h with intermittent grindings. Samples prepared by both techniques gave similar results. In either case the samples after the firing schedule were allowed to cool in the furnace by turning off the power. These samples are designed "as-prepared samples." The as-prepared samples were then annealed at different temperatures in a N_2 atmosphere; these samples are designated " N_2 -annealed samples." The N_2 gas from commercial cylinders was passed through a heated copper column to reduce the amount of residual oxygen.

The products were all characterized by x-ray powder diffraction. Lattice parameters were refined using KCl as an internal standard. The oxygen content was determined by iodometric titration.¹² Superconducting transition temperatures were determined with a superconducting quantum interference device (SQUID) magnetometer with a field of 10 Oe.

III. RESULTS AND DISCUSSION

A. Cerium solubility

The solubility limits x_{lim} of Ce in $L_{2-x}Ce_xCuO_4$ were determined by x-ray powder diffraction. The value of x at which impurity phases start appearing in the x-ray-diffraction patterns was taken as the solubility limit of Ce. The variation of the Ce solubility limit with the size of L^{3+} ions is shown in Fig. 1. The Ce solubility decreases monotonically with decreasing size of L^{3+} .

The solubility limits $x_{lim}=0.20$ and 0.15 found, respectively, for $L = Nd$ and Gd in $L_{2-x}Ce_xCuO_4$ agree well with those already reported in the literature.¹³ We have been able to increase the Ce solubility limit to $x_{lim}=0.25$ in $La_{1.3}Nd_{0.45}Ce_{0.25}CuO_4$ or $(La_{0.74}Nd_{0.26})_{1.75}Ce_{0.25}CuO_4$. This is the maximum Ce solubility that one can achieve in the T' structure. The compound $La_{1.3}Nd_{0.45}Ce_{0.25}CuO_4$ has the largest a parameter (3.993 Å) of all the known T' phases, and the corresponding

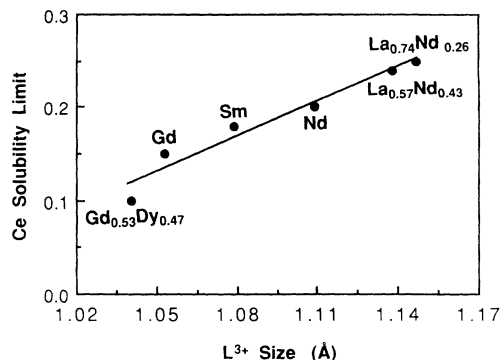


FIG. 1. Variation of Ce solubility limit with the size of the L^{3+} ion in $L_{2-x}Ce_xCuO_4$.

Cu-O bond length of 1.997 Å represents the upper limit for the T' structure. Any attempt to increase the Ce solubility limit beyond $x_{lim}=0.25$ with La content in $La_yNd_{2-y-x}Ce_xCuO_4$ results in the formation of impurity phases having the T structure. Also, near these upper limits of T' phase field, lowering of Ce content below the solubility limit x_{lim} results in the formation of T phases as impurity. For example, $La_{1.3}Nd_{0.45-x}Ce_xCuO_4$ is formed only for a narrow range of $0.20 \leq x \leq 0.25$ and $LaNd_{1-x}Ce_xCuO_4$ for $0.09 \leq x \leq 0.24$. Formation of T phases as impurities near the upper T' phase field is also apparent in a study¹⁴ of $Nd_{1.85-x}La_xCe_{0.15}CuO_4$, in which T -phase impurities are formed for $x > 1.2$.

We also find that the Ce solubility limit decreases to $x_{lim}=0.10$ in $GdDy_{0.9}Ce_{0.1}CuO_4$, or $(Gd_{0.53}Dy_{0.47})_{1.9}Ce_{0.10}CuO_4$. This phase is close to the lower end of the T' phase field. The compound $Gd_{1.4}Dy_{0.6}CuO_4$ — $(Gd_{0.7}Dy_{0.3})_2CuO_4$ —has the smallest a parameter (3.888 Å) of all the known T' phases, and the corresponding Cu-O bond length of 1.944 Å represents the lower limit for the T' structure. Attempts to increase the Dy content further, or to substitute Ce for (Gd,Dy) in $Gd_{1.4}Dy_{0.6}CuO_4$, result in the formation of $L_2Cu_2O_5$ impurity phases. However, the T' phase field can be lowered to smaller $L = Dy, Ho, Er, Tm$, and Y , if high hydrostatic pressure (6 GPa) is used in the synthesis.¹⁵

The decreasing solubility limit of Ce with decreasing size of L^{3+} can be explained on the basis of a bond-length matching criterion. As the size of the L^{3+} ion in the T' L_2CuO_4 increases, the degree of bond-length mismatch and internal stresses increase. The greater the degree of bond-length mismatch, the larger are the number of antibonding electrons that can be introduced into the CuO_2 sheets and/or the larger would be the amount of Ce^{4+} that can be substituted for L^{3+} . Therefore, the Ce solubility increases with increasing size of the L^{3+} ion. Gd_2CuO_4 with a smaller a parameter has a relatively lower degree of internal stresses and a Ce doping level of $x=0.15$ suffices to relieve the internal stresses. On the other hand, $LaNdCuO_4$ with a greater degree of internal stresses requires a Ce doping of $x=0.24$ to relieve the internal stresses. Complete relief of internal stresses at

$x = x_{\text{lim}}$ prohibits further doping by Ce beyond the observed solubility limit. It is now clear that the driving force for n -type doping in $L_{2-x}\text{Ce}_x\text{CuO}_4$ as well as the extent of doping are primarily determined by the degree of internal stresses introduced by bond-length mismatch.

The narrow range of Ce incorporation in $\text{La}_{1.3}\text{Nd}_{0.45-x}\text{Ce}_x\text{CuO}_4$ ($0.20 \leq x \leq 0.25$) and $\text{LaNd}_{1-x}\text{Ce}_x\text{CuO}_4$ ($0.09 \leq x \leq 0.24$) needs further comment. These phases are near the upper limit of the T' phase field. Any increase in L -O bond length would increase the tolerance factor t and favor the stabilization of T phases. Lowering of Ce content to $x < 0.20$ in $\text{La}_{1.3}\text{Nd}_{0.45-x}\text{Ce}_x\text{CuO}_4$ or $x < 0.09$ in $\text{LaNd}_{1-x}\text{Ce}_x\text{CuO}_4$ increases the average (L,Ce) -O bond length in the $(L,\text{Ce})_2\text{O}_2$ layer and renders the T' structure unstable.

B. Oxygen content

The as-prepared samples of $L_{2-x}\text{Ce}_x\text{CuO}_{4+\delta}$ all have $\delta \approx 0.02$ excess oxygen. The excess δ oxygen occupy the empty octahedral positions of the $L_{2-x}\text{Ce}_x\text{O}_2$ fluorite layer—i.e., the (0.5,0.5,0.3523) sites in the $I4/mmm$ space group of the T' structure—and create randomly five-coordinated Cu. A nonuniform oxygen coordination perturbs the periodic potential of the CuO_2 sheets and causes a trapping of the carriers within the mobility edge, which gives rise to semiconducting behavior.¹⁶ Therefore, annealing of $L_{2-x}\text{Ce}_x\text{CuO}_{4+\delta}$ in N_2 atmosphere at higher temperatures is essential to remove the excess interstitial oxygen atoms and to induce superconductivity. However, there appears to be an equilibrium between the oxygen atoms occupying the normal tetrahedral sites and the interstitial octahedral sites, which necessitates creation of a small, but sufficient, number of oxygen vacancies in the tetrahedral sites before all the interstitial oxygen atoms can be removed.¹⁷ We find from careful iodometric titration on a number of samples that an oxygen-vacancy concentration $\delta \geq 0.01$ in $L_{2-x}\text{Ce}_x\text{CuO}_{4-\delta}$ is necessary to remove all the interstitial oxygen atoms and induce superconductivity with a strong Meissner signal. We ascertain, as has been broadly suggested in the literature,^{18,19} that creation of oxygen vacancies in $L_{2-x}\text{Ce}_x\text{CuO}_{4-\delta}$ is an essential factor to achieve superconductivity.

We find that the oxygen content generally decreases with increasing N_2 -annealing temperature as one would expect. For a constant N_2 -annealing temperature, the total oxygen content increases with increasing cerium content (Fig. 2). The results shown in Fig. 2 for the system $\text{LaNd}_{1-x}\text{Ce}_x\text{CuO}_{4-\delta}$ are obtained after annealing at a constant temperature of 950°C in N_2 . An oxygen-vacancy concentration $\delta = 0.03$ is found for $x = 0.09$ whereas $\delta \approx 0.00$ is found for $x = 0.22$. It becomes increasingly difficult to create oxygen vacancies as the cerium content increases; no oxygen vacancies are found near the Ce solubility limit. This finding has important consequences, as we show in the next section; to our knowledge, this effect has not been established in the literature. We believe that the lack of such information is due to the decreasing solubility of $L_{2-x}\text{Ce}_x\text{CuO}_{4-\delta}$ in a mixture of KI and HCl during the iodometric analysis as

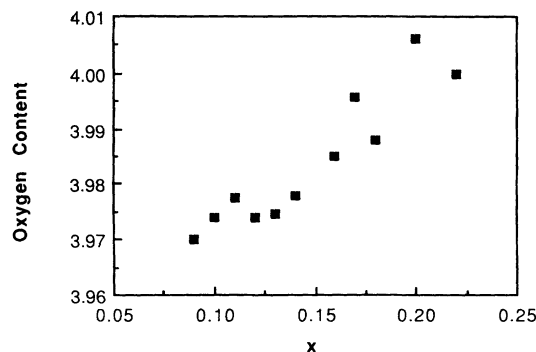


FIG. 2. Variation of oxygen content in $\text{LaNd}_{1-x}\text{Ce}_x\text{CuO}_4$ with x for a constant annealing temperature of 950°C in N_2 atmosphere.

the L^{3+} size decreases. The decreasing basicity of smaller L^{3+} ions appears to decrease the dissolution; similar results are found in several other systems.²⁰ The difficulties in sample dissolution as well as the limited Ce solubility for smaller $L = \text{Pr}, \text{Nd}, \text{Sm}, \text{and Eu}$ might have hindered the observation of a small, but systematic, variation of oxygen content with cerium content. With the larger $L = (\text{La}, \text{Nd})$ in $\text{LaNd}_{1-x}\text{Ce}_x\text{CuO}_{4-\delta}$, we could precisely determine the oxygen content and notice clearly the variation of oxygen content with Ce content.

The monotonic increase in oxygen content, or decrease in oxygen vacancies, with increasing Ce content can be explained on the basis of the degree of internal stresses introduced by bond-length mismatch. Creation of oxygen vacancies in $L_{2-x}\text{Ce}_x\text{CuO}_{4-\delta}$ introduces antibonding electrons into the CuO_2 sheets, which can relieve the tensile stress in the Cu-O bonds. Also, oxygen vacancies in the $(L,\text{Ce})_2\text{O}_{2-\delta}$ fluorite layer can reduce the electrostatic repulsion between the O^{2-} ions and the compressive stress in the (L,Ce) -O bonds. The decreasing degree of internal stresses with increasing Ce content results in a decreasing driving force for the acceptance of antibonding electrons and oxygen-vacancy concentration. Close to the solubility limit $x \approx 0.24$ in $\text{LaNd}_{1-x}\text{Ce}_x\text{CuO}_4$, the internal stresses have nearly been relieved and it becomes difficult to create any oxygen vacancies. Also, the increasing concentration of Cu^+ with Ce content makes it increasingly difficult to create additional Cu^+ via the creation of oxygen vacancies, because Cu^+ generally prefers linear or tetrahedral oxygen coordination; thus it is somewhat difficult to keep large concentrations of Cu^+ in square-coplanar oxygen coordination.

The synthesis of $\text{Nd}_{2-y-x}\text{La}_y\text{Ce}_x\text{CuO}_4$ for $0 \leq y \leq 1.0$ has also enabled us to monitor the variation of oxygen content with the size of L^{3+} for a fixed Ce content and a given N_2 -annealing temperature. The variation of oxygen content with L^{3+} size or with the a parameter is shown in Fig. 3 for $\text{Nd}_{2-y-0.12}\text{La}_y\text{Ce}_{0.12}\text{CuO}_4$ ($0 \leq y \leq 1.0$). These samples with a fixed Ce content $x = 0.12$ were all annealed in N_2 at 950°C and were analyzed for oxygen content. We find a small, but steady, increase in the total oxygen content, or a decrease in the oxygen vacancies, as

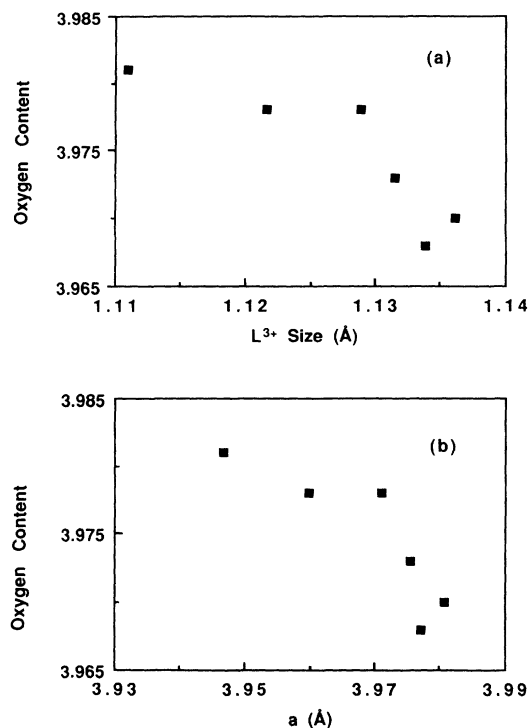


FIG. 3. Variation of oxygen content in $\text{Nd}_{2-y-0.12}\text{La}_y\text{Ce}_{0.12}\text{CuO}_4$ ($0 \leq y \leq 1.0$) with (a) the size of the L^{3+} ion and (b) the a parameter for a constant annealing temperature of 950°C in N_2 atmosphere.

the average size of L^{3+} decreases. To our knowledge this systematic variation has not been described in the literature; we show in the next section the consequences of such a variation.

The decreasing oxygen-vacancy concentration with decreasing size of L^{3+} for a fixed Ce concentration is again due to the decreasing degree of bond-length mismatch. Similar arguments have also been made²¹ to account for the decreasing degree of self-doping with decreasing L^{3+} size in the undoped $\text{L}_2\text{CuO}_{4-\delta}$ oxides. In addition, the less basic, smaller L^{3+} ions become more strongly bound to the oxygen atoms, with an increase in covalent character. A stronger bonding between the smaller L^{3+} and O^{2-} ions can make the removal of oxygen atoms from the tetrahedral sites of the L_2O_2 fluorite layers difficult.

C. Carrier concentration and superconductivity

The variation of T_c with Ce content x is shown in Fig. 4 for $\text{LaNd}_{1-x}\text{Ce}_x\text{CuO}_{4-\delta}$ and $\text{Nd}_{2-x}\text{Ce}_x\text{CuO}_{4-\delta}$. Samples with compositions in the shaded regions exhibited a much reduced Meissner signal and consist of two-phase regions of the antiferromagnetic semiconductor and superconducting phases. The value of x at which superconductivity begins with a maximum Meissner signal is designated as the critical value x_c of Ce concentration required for a transition from the antiferromagnetic semiconductor to the superconductor; for $x \geq x_c$, the Meissner signal remains nearly constant for all the superconductive compositions. We notice from Fig. 4 that the

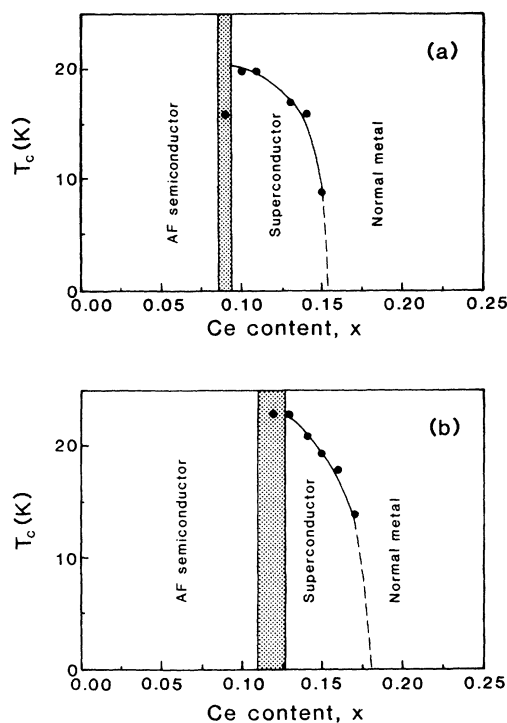


FIG. 4. Variation of T_c with Ce concentration x for (a) $\text{LaNd}_{1-x}\text{Ce}_x\text{CuO}_4$ and (b) $\text{Nd}_{2-x}\text{Ce}_x\text{CuO}_4$. The shaded area represents a two-phase region between the antiferromagnetic semiconductor and the superconductor regions. For the sake of comparison, the abscissa has been maintained from $x=0.0$ to $x=0.25$ in both the systems, but the phases are formed only for $0.09 \leq x \leq 0.24$ in $\text{LaNd}_{1-x}\text{Ce}_x\text{CuO}_4$ and $0 \leq x \leq 0.20$ in $\text{Nd}_{2-x}\text{Ce}_x\text{CuO}_4$.

value of x_c increases from 0.10 in $\text{LaNd}_{1-x}\text{Ce}_x\text{CuO}_{4-\delta}$ to 0.13 in $\text{Nd}_{2-x}\text{Ce}_x\text{CuO}_{4-\delta}$. This difference is significant and could be attributed⁸ to an increasing Madelung energy caused by a decreasing a parameter on going from $\text{LaNd}_{1-x}\text{Ce}_x\text{CuO}_{4-\delta}$ to $\text{Nd}_{2-x}\text{Ce}_x\text{CuO}_{4-\delta}$. The decreasing a parameter reduces the Cu-O bond length and can increase the Madelung energy, which is inversely proportional to the Cu-O distance. An increasing Madelung energy can raise the Cu 3d energies and increase the charge-transfer gap Δ between the Cu 3d and O 2p bands.²² In fact, from optical measurements the charge-transfer gap Δ has been shown²³ experimentally to increase monotonically on passing from $L=\text{Pr}$ to $L=\text{Gd}$. An increasing Δ will reduce the covalent mixing parameter

$$\lambda = b^{ca} / \Delta, \quad (2)$$

where b^{ca} is the cation-anion resonance integral; this can necessitate a higher level of doping for superconductivity to occur. We proposed this interpretation previously,⁸ based on the assumption that the oxygen content for a given N_2 -annealing temperature remains constant for all concentrations x of cerium, irrespective of the size of the L^{3+} ions. Our present assertion is that the oxygen con-

tent is variable, depending on the size of L^{3+} and the Ce content; this made us reexamine our position.

We prepared several samples in the $L_{2-x}\text{Ce}_x\text{CuO}_4$ system for $L = \text{Nd}_{1-y}\text{La}_y$, Nd, Sm, and Gd. The critical value x_c is plotted against the experimentally observed a parameter and the L^{3+} size in Fig. 5. The value of x_c increases with decreasing size of the L^{3+} ion as one would expect, based on our previous results⁸ with $\text{LaNd}_{1-x}\text{Ce}_x\text{CuO}_{4-\delta}$ and $\text{Nd}_{2-x}\text{Ce}_x\text{CuO}_{4-\delta}$. However, the critical electron concentration n_c in the CuO_2 sheets required to induce a transition from antiferromagnetic semiconductor to superconductor seems to remain nearly constant at $n_c = 0.175 \pm 0.005$ for all L^{3+} ion sizes or a parameters (Fig. 6). The n_c values were calculated from the experimentally observed oxygen content, assuming L^{3+} , Ce^{4+} , and O^{2-} valences in the solid $L_{2-x}\text{Ce}_x\text{CuO}_{4-\delta}$ samples. The experimental error in the determination of oxygen is ± 0.005 and the corresponding experimental error in n_c is ± 0.01 . The observed n_c values in Fig. 6 remain constant within this experimental error bar. The n_c value for smaller $L = \text{Sm}$ is not included in Fig. 6 because of the possible error in the oxygen content, which arises from the decreasing solubility during iodometric titration, and formation of impurity phases during N_2 -annealing. A decreasing degree of tensile stress in the Cu-O bonds with decreasing size of L^{3+} ions makes it increasingly difficult to create and sustain oxygen vacancies; thus, the samples with smaller L^{3+} ions tend to decompose during N_2 annealing. This problem becomes severe with the still smaller $L = \text{Gd}$, and the

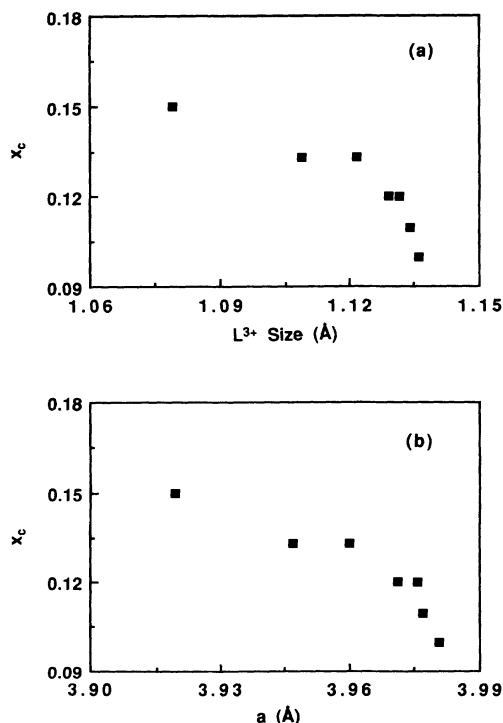


FIG. 5. Variation with (a) the size of the L^{3+} ion and (b) the a parameter of the critical Ce concentration x_c that is required to induce a transition from antiferromagnetic semiconductor to superconductor in $\text{Nd}_{2-y-x}\text{La}_y\text{Ce}_x\text{CuO}_4$ ($0 \leq y \leq 1.0$) and $\text{Sm}_{2-x}\text{Ce}_x\text{CuO}_4$.

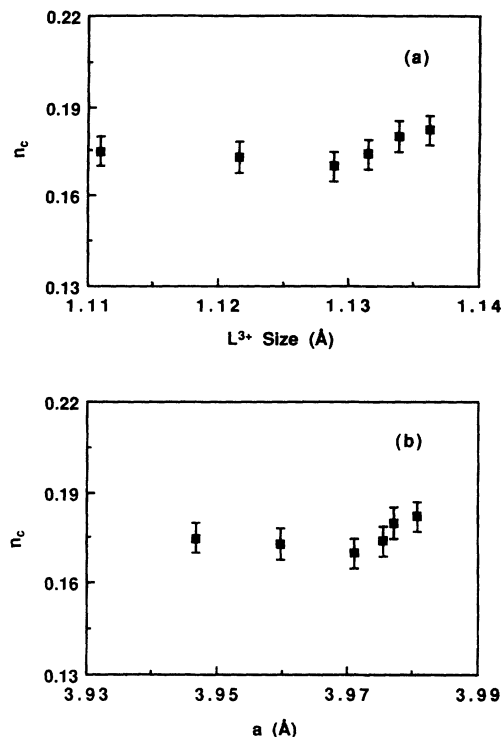


FIG. 6. Variation with (a) the size of the L^{3+} ion and (b) the a parameter of the critical electron concentration n_c that is required to induce a transition from antiferromagnetic semiconductor to superconductor in $\text{Nd}_{2-y-x}\text{La}_y\text{Ce}_x\text{CuO}_4$ ($0 \leq y \leq 1.0$).

$\text{Gd}_{2-x}\text{Ce}_x\text{CuO}_4$ samples decompose rapidly to give Cu_2O , as indicated by a color change from black to brown.

It is clear from our present data that the transition from antiferromagnetic semiconductor to superconductor in $L_{2-x}\text{Ce}_x\text{CuO}_4$ occurs at a nearly fixed electron concentration $n_c = 0.175 \pm 0.005$, irrespective of the size of L^{3+} ions or the a parameter. The apparent increase in the value of x_c with decreasing L^{3+} ion size is due to the decreasing number of oxygen vacancies with the decreasing size of the L^{3+} ion. We conclude that the influence of Madelung energy or charge-transfer gap Δ is less significant in determining the critical amount of doping necessary to induce a transition from antiferromagnetic semiconductor to superconductor.

The present data also can explain why one does not observe superconductivity in $\text{Gd}_{2-x}\text{Ce}_x\text{CuO}_4$ at $x = 0.15$. The smaller Gd^{3+} ion limits the Ce solubility to $x_{\text{lim}} = 0.15$ (Fig. 1). The electron concentration $n = 0.15$ at $x_{\text{lim}} = 0.15$, assuming an oxygen content of 4.00, is much less than the n_c value of 0.175 ± 0.005 required to induce superconductivity. Although n can further be increased in other systems with larger L^{3+} ions via the creation of oxygen vacancies, such a mechanism does not seem to work with the smaller $L = \text{Gd}$. A stronger bonding between smaller Gd^{3+} and O^{2-} ions, and a nearly complete relief of the internal stresses near the Ce solubil-

ity limit $x_{\text{lim}} = 0.15$ in $\text{Gd}_{1.85}\text{Ce}_{0.15}\text{CuO}_4$, make it difficult to create oxygen vacancies in this compound.

IV. CONCLUSION

The internal stresses introduced by a bond-length mismatch between the (L,Ce)-O and Cu-O bonds have important influences on the crystal chemistry, chemical composition, and properties of $L_{2-x}\text{Ce}_x\text{CuO}_4$. The consequences of the internal stresses have been investigated systematically by varying the size of the L^{3+} ions. The results are summarized below.

(1) The Ce solubility limit decreases with decreasing size of L^{3+} ions.

(2) The oxygen content increases, or the oxygen-vacancy concentration decreases, with decreasing size of L^{3+} ion for a given N_2 -annealing temperature and Ce content. For a given L^{3+} ion and N_2 -annealing tempera-

ture, the oxygen content increases with increasing Ce content.

(3) The transition from antiferromagnetic semiconductor to superconductor in $L_{2-x}\text{Ce}_x\text{CuO}_4$ seems to occur at a nearly fixed critical electron concentration $n_c = 0.175 \pm 0.005$. However, a decreasing concentration of oxygen vacancies with decreasing size of L^{3+} causes an increase in the critical Ce concentration x_c required to induce the transition.

ACKNOWLEDGMENTS

Financial support by the Robert A. Welch Foundation Grant No. F-1254 and the National Science Foundation Grant No. DMR-9223552 is gratefully acknowledged. Support by the National Science Foundation Grant No. DMR-9109080 for the acquisition of a SQUID magnetometer is also gratefully acknowledged.

¹M. Takano, Y. Takeda, H. Okada, M. Miyamoto, and K. Kusaka, *Physica C* **159**, 375 (1989).

²M. G. Smith, A. Manthiram, J. Zhou, J. B. Goodenough, and J. T. Markert, *Nature* **351**, 549 (1991).

³J. B. Goodenough, *Supercond. Sci. Technol.* **3**, 26 (1990).

⁴J. B. Goodenough and A. Manthiram, *J. Solid State Chem.* **88**, 115 (1990).

⁵R. D. Shannon, *Acta Crystallogr. A* **32**, 751 (1976).

⁶A. Manthiram and J. B. Goodenough, *J. Solid State Chem.* **92**, 231 (1991).

⁷A. Manthiram and J. B. Goodenough, *J. Solid State Chem.* **87**, 402 (1990).

⁸A. Manthiram, *J. Solid State Chem.* **100**, 383 (1992).

⁹Y. K. Tao, M. Bonvalot, Y. Y. Sun, R. L. Meng, P. H. Hor, and C. W. Chu, *Physica C* **165**, 13 (1990).

¹⁰H. Takagi, S. Uchida, and Y. Tokura, *Phys. Rev. Lett.* **62**, 1197 (1989).

¹¹N. Y. Ayoub, J. T. Markert, E. A. Early, C. L. Seaman, L. M. Paulius, and M. B. Maple, *Physica C* **165**, 469 (1990).

¹²A. Manthiram, J. S. Swinnea, Z. T. Sui, H. Steinfink, and J. B. Goodenough, *J. Am. Chem. Soc.* **109**, 6667 (1987).

¹³T. C. Huang, E. Moran, A. I. Nazzari, and J. B. Torrance, *Physica C* **158**, 148 (1989).

¹⁴E. Wang, J.-M. Tarascon, L. H. Greene, and G. W. Hull, *Phys. Rev. B* **41**, 6582 (1990).

¹⁵H. Okada, M. Takano, and Y. Takeda, *Phys. Rev. B* **42**, 6813 (1990).

¹⁶A. Manthiram, X. X. Tang, and J. B. Goodenough, *Phys. Rev. B* **42**, 138 (1990).

¹⁷Y. T. Zhu and A. Manthiram (unpublished).

¹⁸R. L. Fuller, K. V. Ramanujachary, and M. Greenblatt, *Mater. Res. Bull.* **27**, 205 (1992).

¹⁹E. Takayama-Muromachi, F. Izumi, Y. Uchida, K. Kato, and H. Asano, *Physica C* **159**, 634 (1989).

²⁰A. Manthiram (unpublished).

²¹J.-S. Zhou, J. Chan, and J. B. Goodenough, *Phys. Rev. B* **47**, 5477 (1993).

²²J. B. Goodenough, J.-S. Zhou, and J. Chan, *Phys. Rev. B* **47**, 5275 (1993).

²³T. Arima, K. Kikuchi, M. Kasuya, S. Koshihara, and Y. Tokura, *Phys. Rev. B* **44**, 917 (1991).